applied sciences

MDPI

Article

Regional Geochemical Characteristics of Lithium in the Mufushan Area, South China

Peiyu Li [1], Qingjie Gong [1,*], Shaoyu Chen [1], Peng Li [2], Jiankang Li [2], Xuan Wu [3], Xiaolei Li [3], Xuefeng Wang [4] and Ningqiang Liu [1]

[1] School of Earth Sciences and Resources, China University of Geosciences, Beijing 100083, China; peiyuli@email.cugb.edu.cn (P.L.); shaoyuchen@email.cugb.edu.cn (S.C.); lnqcug@cugb.edu.cn (N.L.)
[2] MNR Key Laboratory of Metallogeny and Mineral Resource Assessment, Institute of Mineral Resources, Chinese Academy of Geological Sciences, Beijing 100037, China; lipeng031111@163.com (P.L.); li9968@126.com (J.L.)
[3] Center for Development and Research, China Geological Survey, Beijing 100037, China; wxuan@mail.cgs.gov.cn (X.W.); lxiaolei@mail.cgs.gov.cn (X.L.)
[4] School of Gemology, China University of Geosciences, Beijing 100083, China; xfwang@email.cugb.edu.cn
* Correspondence: qjiegong@cugb.edu.cn

Abstract: With the explosive growth in demand for lithium (Li) resources, the Mufushan area has been a hotspot for Li deposit exploration in China in recent years. Geochemical maps and geochemical anomaly maps are basic maps in the geochemical exploration of mineral resources. A fixed-value method to contour a Li geochemical map is presented here, in which Li concentrations are divided into 19 levels on 18 fixed values, ranging from 5 μg/g (corresponding to the detection limit) to 1858 μg/g (corresponding to the cut-off grade of Li deposit in hard-rock type) and illustrated in six color tones corresponding to Li areas of low background, high background, low anomaly, high anomaly, mineralization in clay-type, and mineralization in hard-rock type. The geochemical map of Li in the Mufushan area using the new fixed-value method indicates that the study area belongs to the high background area, and the known Li deposits are located in the high anomaly areas. In addition, the geochemical anomaly map of the Mufushan area is drawn using the method of seven levels of classification, and indicates that the known Li deposits are all in the anomaly areas, with anomaly levels not lower than the second level. Furthermore, four other areas are recognized for Li resource potential based on the geochemical map and geochemical anomaly map in the Mufushan area.

Keywords: Li resource potential; fixed-value method; 19 levels of geochemical map; seven levels of classification; Mufushan area

check for updates

Citation: Li, P.; Gong, Q.; Chen, S.; Li, P.; Li, J.; Wu, X.; Li, X.; Wang, X.; Liu, N. Regional Geochemical Characteristics of Lithium in the Mufushan Area, South China. *Appl. Sci.* **2024**, *14*, 1978. https://doi.org/10.3390/app14051978

Academic Editor: Nikolaos Koukouzas

Received: 30 January 2024
Revised: 13 February 2024
Accepted: 27 February 2024
Published: 28 February 2024

1. Introduction

Lithium (Li) is a crucial element in today's world, primarily due to its significant role in the production of batteries for the electronic devices. Li deposits of various types are widely distributed across the globe. Among them, salt lake Li deposits and pegmatite-type Li deposits still dominate. Salt lake lithium mines are concentrated in the region of South America, centered on Chile, Argentina, and Bolivia. Pegmatite lithium mines are concentrated in Africa and Western Australia [1–4]. Li resources are rich in China, but the exploration of Li deposits is infrequent [5,6]. The Mufushan area is a representative Li mineralization area in south China, which has been a hotspot area of Li resource exploration recently [7–11].

The Regional Geochemistry–National Reconnaissance (RGNR) project has been implemented since 1979 and has covered >7 million square kilometers of Chinese land surface [12,13]. These regional geochemical survey data were compiled to form a RGNR database [14]. The Multi-Purpose Regional Geochemistry Survey (NMPRGS) project was initiated in 1999 and has been carried out in the agriculturally and industrially developed regions of China [15]. Geochemical maps and geochemical anomaly maps drawn from these data have been basic maps in the geochemical exploration of mineral resources and basic geological surveys [16–19]. With respect to the geochemical map, a new mapping technique called the fixed-value method was presented and illustrated on Cr and Sn, which can overcome the flaw of dependence on the amount of data [20,21]. The fixed values fully consider the current domestic and international classification, or statistical parameters of element concentrations. When a suitable grading value is unavailable, interpolation among adjacent values is used [21]. However, the fixed-value method on Li geochemical mapping has not been proposed.

With respect to the geochemical anomaly map, a new method called seven levels of classification was presented, which is an objective, distribution free, multivariate, and unfixed method on elemental anomalies [22–24]. In the method of seven levels of classification, two parameters of each trace element, cutoff grade (C_g) and background value (C_b), are used to determine and classify its geochemical anomalies. The empirical equations proposed by Gong et al. [24] and Chen et al. [23] can describe the respective background values (C_b) of each sample, and the seven-level anomaly is based on the respective background values of each sample and the cutoff grade (C_g) of the elements to classify the anomaly level of the sample into seven levels. Seven levels numbered 0, 1, 2, . . ., 6 are divided equally for the difference between $\lg C_g$ and $\lg C_b$ (or between C_g and C_b for Zr, where "lg" stands for logarithm). For an analyzed concentration of a trace element in a sample, (a) if the analyzed concentration is not less than the C_g, its anomaly level is set to a value of 7, (b) if the concentration is less than its C_b in the sample, its anomaly level is assigned a value of −1, (c) if the concentration is located at the values of levels 0 and 1, its anomaly level is set as 0, (d) if the concentration is within the values of levels of 1 and 2, its anomaly level is set as 1, and so on. For this method, the C_g is a fixed value for a trace element, while the C_b is an unfixed value which is dependent on the sample. That is to say, the method of seven levels of classification is applicable to a sample and is not constrained by the amount of data (or samples) [22].

In this paper, the Mufushan area was selected to explore the Li resources on the geochemical map and geochemical anomaly map of Li, based on the data from the RGNR project. Firstly, the fixed-value method for Li was proposed to contour the geochemical map of Li. Then, the seven levels of classification method was adopted to draw the geochemical anomaly map of Li. Finally, the Li mineralization potential in the Mufushan area was discussed, derived from the geochemical map and geochemical anomaly map.

2. Materials and Methods

2.1. Geological Settings

The Mufushan area is situated on the borders between Hunan, Jiangxi, and Hubei provinces in China, and has an area of ca. 13,750 km^2 (Figure 1) ranging from E 113°10′ to E 114°19′, and from N 28°35′ to N 29°43′, in this study, and is in a subtropical monsoon climate zone with humid climate. The average annual temperature is ca. 11 °C and the annual rainfall is ca. 1979 mm, most of which falls in summer according to the public network data. The topography in the Mufushan area is characterized by mountainous and hilly regions, with the main peak reaching an elevation of 1599 m.a.s.l. Soils are thinly developed, and the regolith thickness commonly varies from 0.5 to 5 m depending on the relief.

The strata are mainly Neoproterozoic basement rock series, Paleozoic and Mesozoic sedimentary rock series, and Cenozoic alluvial sands [25]. The Neoproterozoic base rock series is mainly the Lengjiaxi Group, which is a set of low-grade metamorphic rocks such as sandy silty slate, metamorphic siltstone, and metamorphic complex sandstone. Sedimentary rocks are mainly distributed from northeast to southwest, and the main lithology is limestone, dolomite, siliceous rocks, sandstone, and siltstone. The alluvial sands are also distributed from northeast to southwest [25]. The lithology of these strata is described briefly in Figure 1.

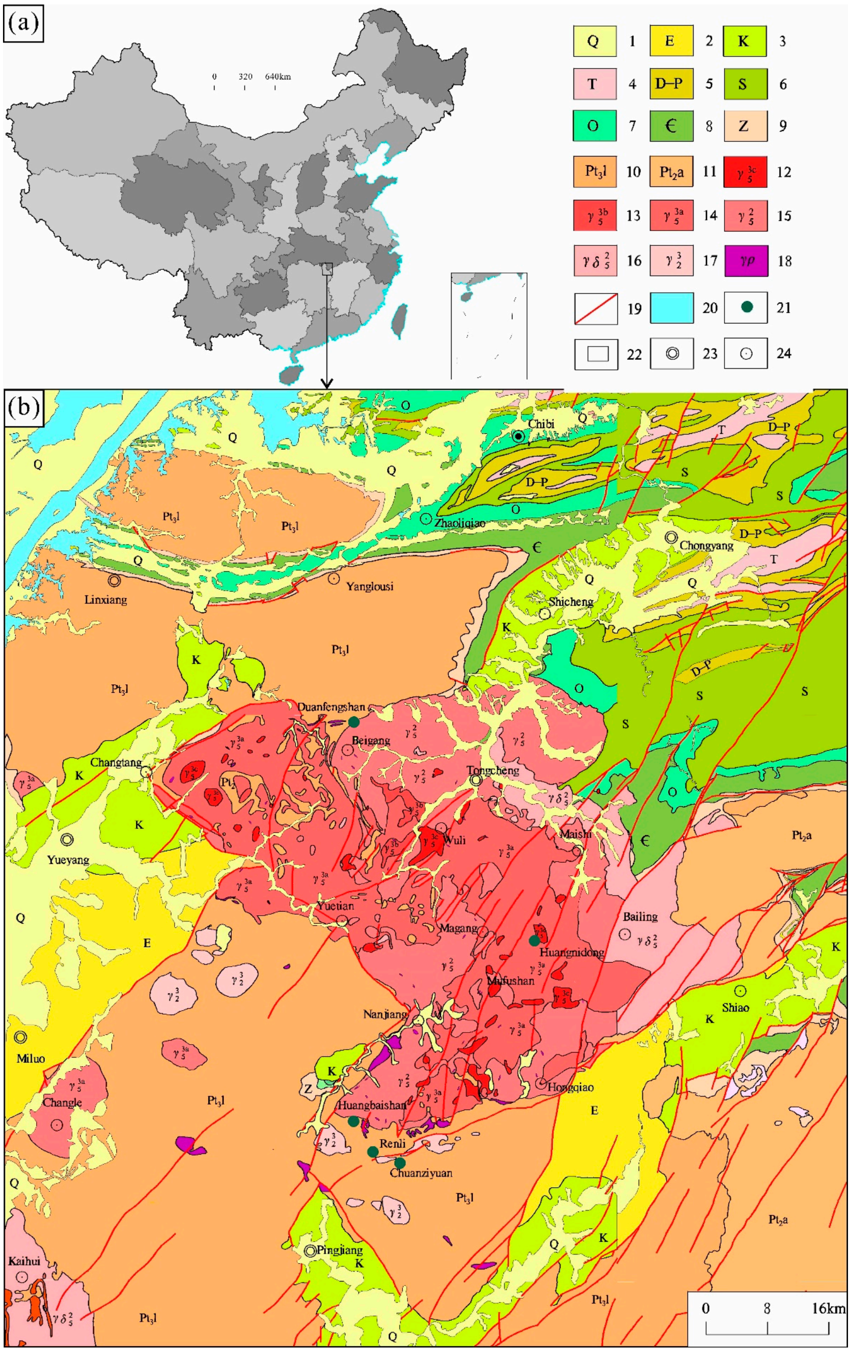

Figure 1. Location of the Mufushan studied area in China (**a**) and its geological map sketched after the H49 and H50 geological map from China Geological Survey (**b**). 1—Quaternary gravel, clay, sub sandy soil, and sub clay; 2—Tertiary conglomerate sandstone and quartz sandstone; 3—Cretaceous sandstone and gravel rock; 4—Triassic limestone, dolomite, and shale; 5—Devonian–Permian limestone, sandstone, siltstone, and shale; 6—Silurian silty shale, argillaceous sandstone, and fine sandstone; 7—Ordovician slate, shale, and siliceous rock; 8—Cambrian limestone, dolomite, siltstone, and shale; 9—Sinian siliceous rocks, carbonaceous shale, and limestone; 10—Neoproterozoic Lengjiaxi Group slate, sandstone, phyllite, and metamorphic siltstone; 11—Mesoproterozoic Anlelin Formation tuff, tuffaceous slate, tuffaceous sandstone, and siltstone; 12—Late Yanshanian granite third stage intrusion; 13—Late Yanshanian granite second stage intrusion; 14—Late Yanshanian granite first stage intrusion; 15—Early Yanshanian granite; 16—Early Yanshanian granodiorite; 17—Neoproterozoic two-mica plagioclase granite; 18—pegmatite; 19—fault; 20—water system; 21—Li deposit; 22—study area; 23—county; 24—township.

Faults are very common in the study area, mainly trending N–E, NE–E, and N–W. The main N–E faults are the Yuetian–Wuli–Tongcheng fault and the Nanjiang–Magang–Maishi fault in the center of the area. The main NE–E fault is the Renli–Hongqiao–Shiao fault in the southeast and the main N–W fault is the Nanjiang–Yuetian–Changtang fault (Figure 1b).

The magmatic activity is extensive in the area, with a granite outcrop area of ca. 2350 km^2. The Mufushan complex granite batholith is the main part of the regional magmatic rocks, and the main lithology is biotite granodiorite, two-mica monzogranite, and muscovite granite [26,27] with multiple evolution stages [28]. The early Yanshanian granodiorites ($\gamma\delta_5{}^2$) are mainly located in the eastern area of the Mufushan complex and the early Yanshanian granites ($\gamma_5{}^2$) are mainly situated in the northeastern and the southwestern areas. The first stage of the late Yanshanian granites ($\gamma_5{}^{3a}$) is the main body of the complex, which is distributed in the central and the northwestern areas, while the second and the third stage of the late Yanshanian granites ($\gamma_5{}^{3b}$ and $\gamma_5{}^{3c}$) are exposed sporadically in the complex (Figure 1b). Furthermore, the Neoproterozoic magmatic rocks ($\gamma_2{}^3$) are distributed in the western and southwestern areas [11].

The main metal resource in the Mufushan area is Li, along with Be, Nb, and Ta. The main deposits of Li found are Renli and Chuanziyuan (or Renli–Chuanziyuan) in the southwest, Duanfengshan in the north, and Huangnidong in the center [26–28]. In addition, the Huangbaishan Li-Nb-Ta deposit has been discovered recently in the southwest of the study area [29]. Except for the Huangnidong Li deposit, the other Li deposits are mainly located at the contact zone between the Mufushan complex and the strata of the Lengjiaxi Group.

2.2. Elemental Data of Geochemical Survey

Geochemical survey data in the Mufushan area are from the RGNR Project. Stream sediment is the sampling media (or sample type) on a 1:200,000 scale in this project [30]. Four 1 km^2 sampling grids were combined to create a composite sample. Each composite sample representing 4 km^2 and was analyzed with 39 geochemical analysis items, including Li and the major components (SiO_2, Al_2O_3, Fe_2O_3, K_2O, Na_2O, CaO, MgO, Ti or TiO_2, P or P_2O_5, and Mn or MnO) [23,24]. Duplicate samples were collected and analyzed in 2% to 3% of the total samples.

The major components were determined using X-ray Fluorescence (XRF) spectrometry and Li was determined using the method of Inductively Coupled Plasma Mass Spectrometry (ICP-MS). The detection limits (5, 50, 10, and 10 μg/g for Li, Ti, P, and Mn, respectively, and 0.05% for other major oxides), accuracy ($\leq$0.07–0.13ΔlgC for different concentrations), and precision ($\leq$8–17% in relative standard deviation for different concentrations) of analyses met the requirements of the RGNR project.

The Mufushan area in this study extends 110 km from west to east and 125 km from north to south with an area of 13,750 km^2. A total of 3628 records were retrieved from the RGNR database to draw the geochemical map and geochemical anomaly map of Li in this area.

3. Results and Discussion

3.1. Concentrations of Li

The statistical parameters of Li concentrations from the total of 3628 records (or composite samples) are listed in Table 1. The concentrations of Li vary from 10.2 μg/g to 279 μg/g, with a range more than an order of magnitude. Therefore, the logarithm of Li is used to illustrate its parameters.

Table 1. The statistical parameters of Li and lgLi in the Mufushan area.

Parameters	Data Amount	Minimum	Lower Quartile (Q1)	Median (Q2)	Upper Quartile (Q3)	Maximum	Average (Avg)	Standard Deviation (Std)
Li	3628	10.2	39	47.3	59.1	279	54.8	29.6
lgLi (a)	3628	1.009	1.591	1.675	1.772	2.446	1.700	0.170
lgLi (b)	3458	1.305	1.587	1.668	1.754	2.064	1.677	0.129
Li (c)	3458	20.2	38.6	46.6	56.8	116	47.5	1.35

Note: The unit is μg/g of Li concentrations. (a) All data; (b) outliers excluded; (c) calculated on the lgLi (b).

The values of lgLi of the total of 3628 records in the Mufushan area are shown in Figure 2a as a histogram, along with its box plot according to the illustration of Xu et al. [21]. The box plot is used to show the distribution, focusing on the cumulative frequency, and its typical parameters are listed in Table 1. The histogram focuses on the distribution on the log-normal, with its parameters also listed in Table 1. The distribution of lgLi is close to the normal distribution except for outliers with clearly large values.

In order to delete the outliers, the method of Avg ± 3Std (where Avg and Std are the abbreviations of average and standard deviation) was adopted. That is to say, the outlier data of lgLi were excluded repeatedly when they were outside the range of Avg ± 3Std until no outliers were found. Finally, 3458 records were left. The lgLi data without outliers are illustrated in Figure 2b and their statistical parameters are also listed in Table 1. The average, standard deviation, and median of the 3458 records (outliers excluded) of lgLi are 1.677, 0.129, and 1.668, respectively (Table 1), corresponding to the average and the median of Li concentrations of 47.5 μg/g and 46.6 μg/g.

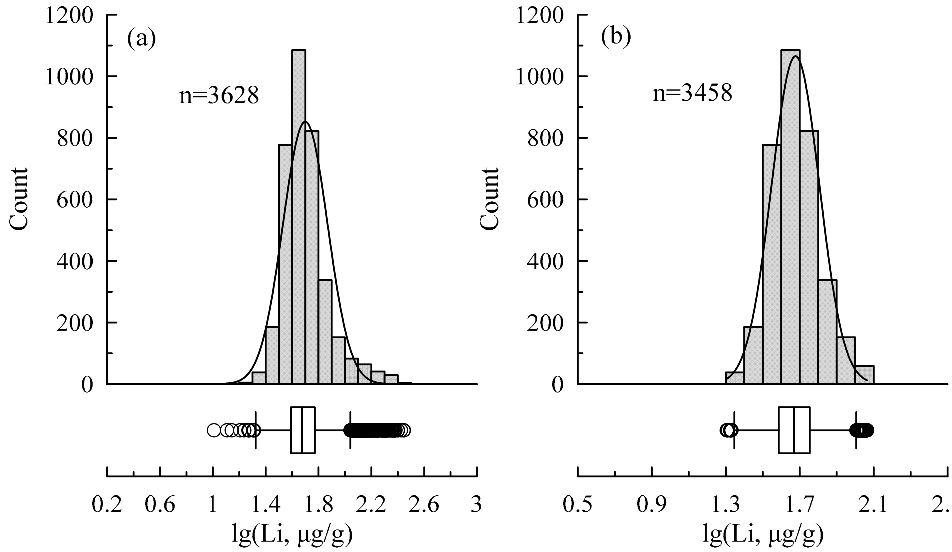

Figure 2. Histograms of Li concentrations with box plots of stream sediments in Mufushan area. (**a**) All data; (**b**) outliers excluded.

3.2. Geochemical Map of Li on Fixed-Value Method

To contour the geochemical map objectively, An et al. [20] and Xu et al. [21] proposed the fixed-value method for Cr and Sn, respectively. According to the construction of the fixed-value method [20,21], a fixed-value method on Li is proposed here on 19 levels according to the method presented by Xu et al. [21] and listed in Table 2 along with the values of the fixed-value method on Sn. In the fixed-value method on Li, to contour the geochemical map, Li concentrations are divided into 19 levels on 18 fixed values which range from 5 μg/g (corresponding to the detection limit) to 1858 μg/g (corresponding to the cut-off grade of Li deposit in hard-rock type).

The first value is 5 μg/g, which is the detection limit of the RGNR project [12,14], although the detection limit of Li was 1 μg/g in the NMPRGS project [31]. The second value is 8 μg/g, which is the 0.5% cumulative frequency value of surface soils in China [32]. The third value is 17 μg/g after the 13 μg/g, corresponding to the 2.5% cumulative frequency value of surface soils in China [32], and 21.5 μg/g, corresponding to the 25% cumulative frequency value of stream sediments in China [14].

The fourth value is 29 μg/g after 27 μg/g, corresponding to the 25% cumulative frequency value of surface soils in China [32] and 30 μg/g, corresponding to the 50% cumulative frequency value of stream sediments in China [14].

The sixth value is set at 40 μg/g after the 40 μg/g, corresponding to the 75% cumulative frequency value of surface soils in China [32], and 40 μg/g of the 75% cumulative frequency value of stream sediments in China [14]. Based on the sixth and fourth values, the fifth value is interpolated as 34 μg/g.

The eighth value is set at 62 μg/g after the 62.2 μg/g, corresponding to the 95% cumulative frequency value of stream sediments in China [14] and 65 μg/g of the 97.5% cumulative frequency value of surface soils in China [32]. Based on the eighth and sixth values, the seventh value is interpolated as 50 μg/g, which is close to the 46.4 μg/g of the 85% cumulative frequency value of stream sediments in China [14].

The twelfth value is 99 μg/g, which is the 99.5% cumulative frequency value of surface soils in China [32]. Based on the twelfth and eighth values, the ninth, tenth, and eleventh values are interpolated as 70 μg/g, 78 μg/g, and 88 μg/g, respectively.

The fifteenth value is 232 μg/g (corresponding to 0.05% of Li_2O), which is the cut-off grade of the clay-type Li deposit [33]. Based on the fifteenth and twelfth values, the thirteenth and fourteenth values are interpolated as 132 μg/g and 175 μg/g, respectively.

The seventeenth value is 930 μg/g (corresponding to 0.2% of Li_2O) which is the cut-off grade of Li as an associated resource [34]. Based on the seventeenth and fifteenth values, the sixteenth value is interpolated as 460 μg/g. The eighteenth value is 1858 μg/g (corresponding to 0.4% of Li_2O) which corresponds to the cut-off grade of the Li deposit in hard-rock type areas [34].

Based on the above 18 fixed values, the concentrations of Li can be classified into 19 levels on the geochemical map of Li. The first level of the 19 levels corresponds to the Li concentration, ranging from the minimum to the first value (or 5 μg/g). The second level of the 19 levels corresponds to the Li concentration ranging from the first value (or 5 μg/g) to second value (or 8 μg/g), and so on. The last level of the 19 levels is corresponding to the Li concentration ranging from the 18th value (or 1858 μg/g) to the maximum, like the description of the fixed values of Sn [21].

In order to better explain these levels, the 19 levels are mapped in six color tones according to those presented by Xu et al. [21]. The levels of first to fifth are the low background areas in blue tones, corresponding to the Li concentrations ranging from the minimum value to 34 μg/g. The levels of sixth to ninth are high background areas in yellow tones, corresponding to concentrations less than 70 μg/g; the tenth to twelfth are low anomaly areas in pink tones less than 99 μg/g; the thirteenth to fifteenth are high anomaly areas in red tones less than 232 μg/g; the sixteenth to eighteenth in gray tones are less than 1858 μg/g, representing the mineralization in clay-type areas; and the nineteenth level is in black, with Li concentrations up to the cut-off grade of Li deposit reflecting the mineralization in hard-rock type areas.

Although the implicit requirement of the ΔlgLi between neighbor levels is not less than 0.1 [21], the fixed-value method of Li constructed here has ΔlgLi values less than 0.1 from the fifth to the twelfth values. This is for two reasons. One is the 19 levels adopted and the other is the two values selected from the Li concentrations of the surface soils and stream sediments in China. The first value is close to the 25% cumulative frequency value of surface soils [32] and the 50% cumulative frequency value of stream sediments [14] in China, and is set as the fourth value of the 19 levels. The second value is the 99.5% cumulative frequency value of surface soils in China [32] and is set as the twelfth value in the 19 levels.

Table 2. The information of the Li geochemical map using the fixed-value method along with those of Sn.

Level No.	0	1	2	3	4	5	6	7	8	9	10	11	12	13	14	15	16	17	18	19	References
Li	min	5	8	17	29	34	40	50	62	70	78	88	99	132	175	232	460	930	1858	max	This study
lgLi	-	0.70	0.90	1.23	1.46	1.53	1.60	1.70	1.79	1.85	1.89	1.94	2.00	2.12	2.24	2.37	2.66	2.97	3.27	-	
ΔlgLi		-	0.20	0.33	0.23	0.07	0.07	0.10	0.09	0.05	0.05	0.05	0.05	0.12	0.12	0.12	0.30	0.31	0.30	-	
Color																					[21]
R		0	9	28	54	128	255	255	255	255	255	255	255	254	249	216	191	135	100	0	
G		0	46	140	224	255	230	223	211	198	229	204	153	92	57	35	191	135	100	0	
B		170	216	248	255	224	153	127	76	25	255	255	255	18	9	0	191	135	100	0	
Sn	min	1	1.3	1.8	2.7	3.4	4.3	6.0	7.9	10	13	17	28	50	100	200	400	600	1000	max	[21]

Note: The concentration unit of Li and Sn is μg/g. The R, G, and B represent the red, green, and blue channels of a color image, respectively.

During the mapping process, the GeoExpl 2013 software [14] was used to grid the original data with a grid spacing of 2 km. The interpolation method was performed using the nearest point model, and the data search mode was a circular domain with a radius of 5 km. The geochemical map was contoured based on the grid data using the fixed-value method of Li and illustrated in Figure 3.

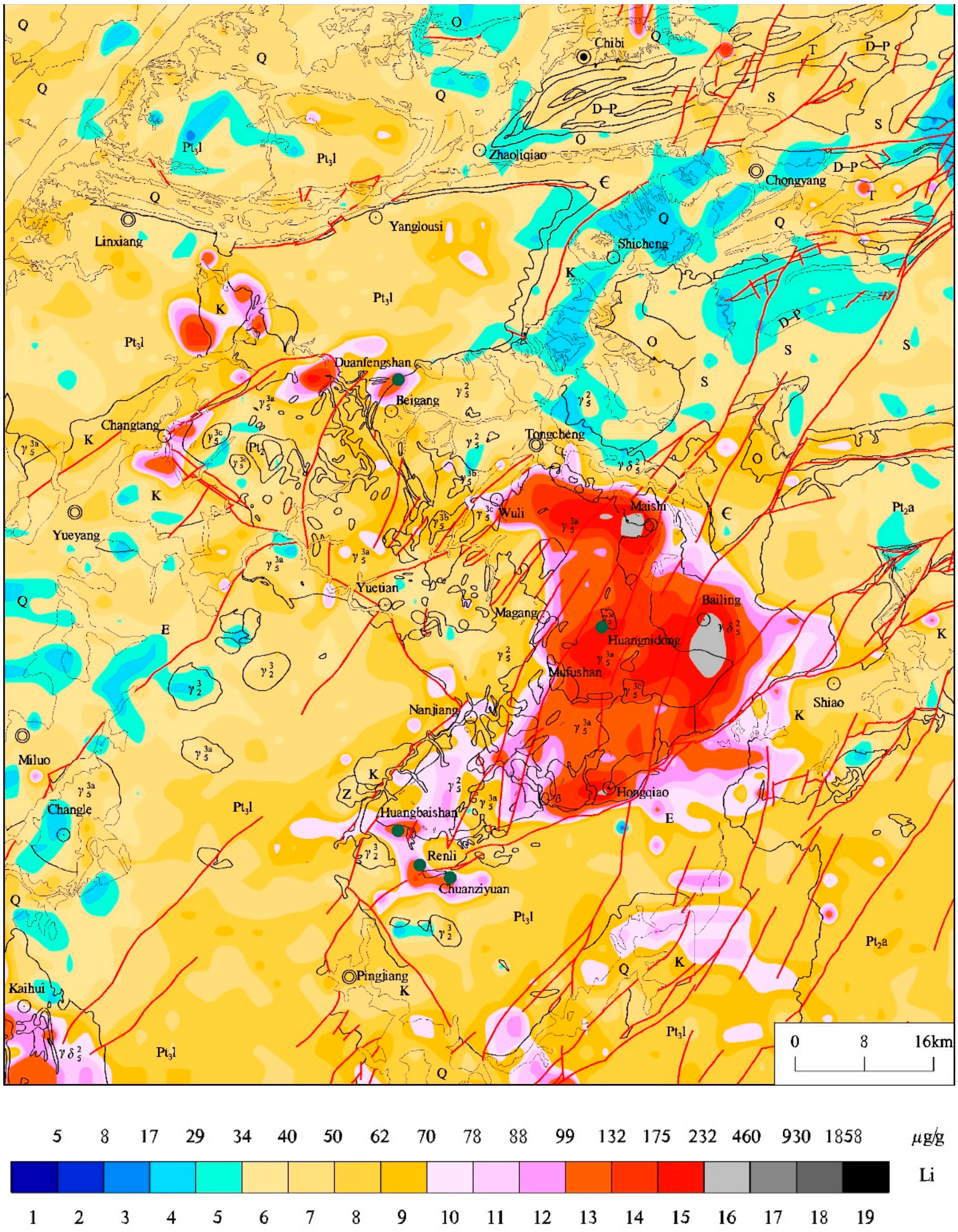

Figure 3. Li geochemical map of Mufushan based on the fixed-value method.

In Figure 3, only 14 levels are illustrated rather than 19 levels because of the Li concentration in the Mufushan area, which ranges from third level to sixteenth level. In Table 1 and Figure 2a, the quartiles of Q1, Q2, and Q3 are colored as the sixth, seventh, and eighth levels in Figure 3, and are located in the high background areas.

The strata and Neoproterozoic intrusions (γ_2^3) are mainly situated in the background areas with blue and yellow tones in Figure 3. With respect to the Mufushan complex, the early Yanshanian granodiorites ($\gamma\delta_5^2$) in the eastern area of the Mufushan complex are mainly in pink, red, and grey tones, indicating the low anomaly, high anomaly, and mineralization in clay-type areas. The early Yanshanian granites ($\gamma_5{}^2$) in the northeastern and the southwestern areas are mainly in yellow, corresponding to the high background areas. The first stage of the late Yanshanian granites ($\gamma_5{}^{3a}$) in the central of the Mufushan complex are mainly in red, indicating the high anomaly areas of Li, while those in the northwestern area are mainly in yellow, reflecting the high background areas. These results indicate that the granitic intrusions of the first stage of the late Yanshanian ($\gamma_5{}^{3a}$) in the central and northwestern parts of the complex may differ in detailed lithology.

The four Li deposits, Duanfengshan in the northern area of the complex, Huangnidong in the central area of the complex, Huangbaishan, and Renli–Chuanziyuan in the southwestern area of the complex, are all located in red, representing the high anomaly areas. Furthermore, three areas with a grey color are recognized at Maishi in the northeastern area of the Mufushan complex, Bailing in the eastern area, and Hongqiao in the southern area of the Mufushan complex, which indicates that the concentrations of Li in these areas are higher than the cut-off grade of Li deposit in clay-type areas [33], or the mineralization in clay-type areas.

3.3. Geochemical Anomaly Map of Li Using Seven Levels of Classification Method

Finding the threshold of anomaly is the key step in drawing a geochemical anomaly map, and it can be determined using a fixed value or unfixed values. With respect to the fixed value of the threshold, the geochemical anomaly map can be viewed as only part of the geochemical map. Therefore, the anomaly areas can also be recognized from high value areas on the geochemical map. However, the elemental concentrations in stream sediments, soils, and rocks are generally dependent on their lithology and weathering degrees [23,24,35,36], so the threshold of anomaly should be determined on unfixed values.

To draw the geochemical anomaly map on unfixed values, Gong et al. [22] proposed a method called seven levels of classification, which adopts a fixed cut-off grade and unfixed backgrounds to classify the elemental concentrations. The determination of elemental background value is the key step in the seven levels of classification method. Although Gong et al. [24] have proposed an empirical equation to describe the backgrounds of Li using samples from some weathering profiles in China, Chen et al. [23] present a new equation using 851 records of elemental abundances including 379, 280, and 192 records of rocks, soils, and stream sediments, respectively, to describe the geochemical backgrounds of Li. Here, the new equation [23] is adopted along with the cut-off grade 1858 μg/g of Li in hard rocks to determine anomalies using the seven levels of classification method in the Mufushan area. The new equation is described as the following, for calculating conveniently.

$$\lg c = -0.02630xy^2z + 0.03000xyz^2 + 0.03540xy + 0.6425y + 3.288 \quad \text{for WIG} < 20 \tag{1}$$

$$\lg c = 0.00001579x^2yz + 0.001141y^2xz - 0.9445y + 0.3650z \quad \text{for } 20 \leq \text{WIG} < 120 \tag{2}$$

$$\lg c = 0.1849xy^2z + 0.03382xyz^2 + 0.6839xyz - 09414x - 1.471y + 1.070z \quad \text{for WIG} \geq 120 \tag{3}$$

where c is the calculated geochemical background of Li in μg/g. The x in Equations (1) and (2) is WIG and is lg(WIG) in Equation (3), where WIG is the weathering index of granite which is calculated in molecular proportions of the major oxides as WIG = 100[Na_2O + K_2O + (CaO-10/3P_2O_5)]/(Al_2O_3 + TFe_2O_3 + TiO_2). The y is lg(Al_2O_3/Ti), where Al_2O_3 and Ti represent their contents with units of wt% and μg/g, respectively. The z is lg(K_2O/SiO_2) where K_2O and SiO_2 represent their contents in wt%.

The anomaly level values of the total of 3628 records are calculated firstly on the GBAL 1.0 software [22], which integrates the new equation to calculate the geochemical backgrounds of Li. Then, the values are gridded to contour the geochemical anomaly map. The gridding parameters such as grid spacing, search radius, and interpolation method are consistent with those in the geochemical map of Li aforementioned. The geochemical anomaly map of Li using the seven levels of classification method in the Mufushan area is illustrated in Figure 4.

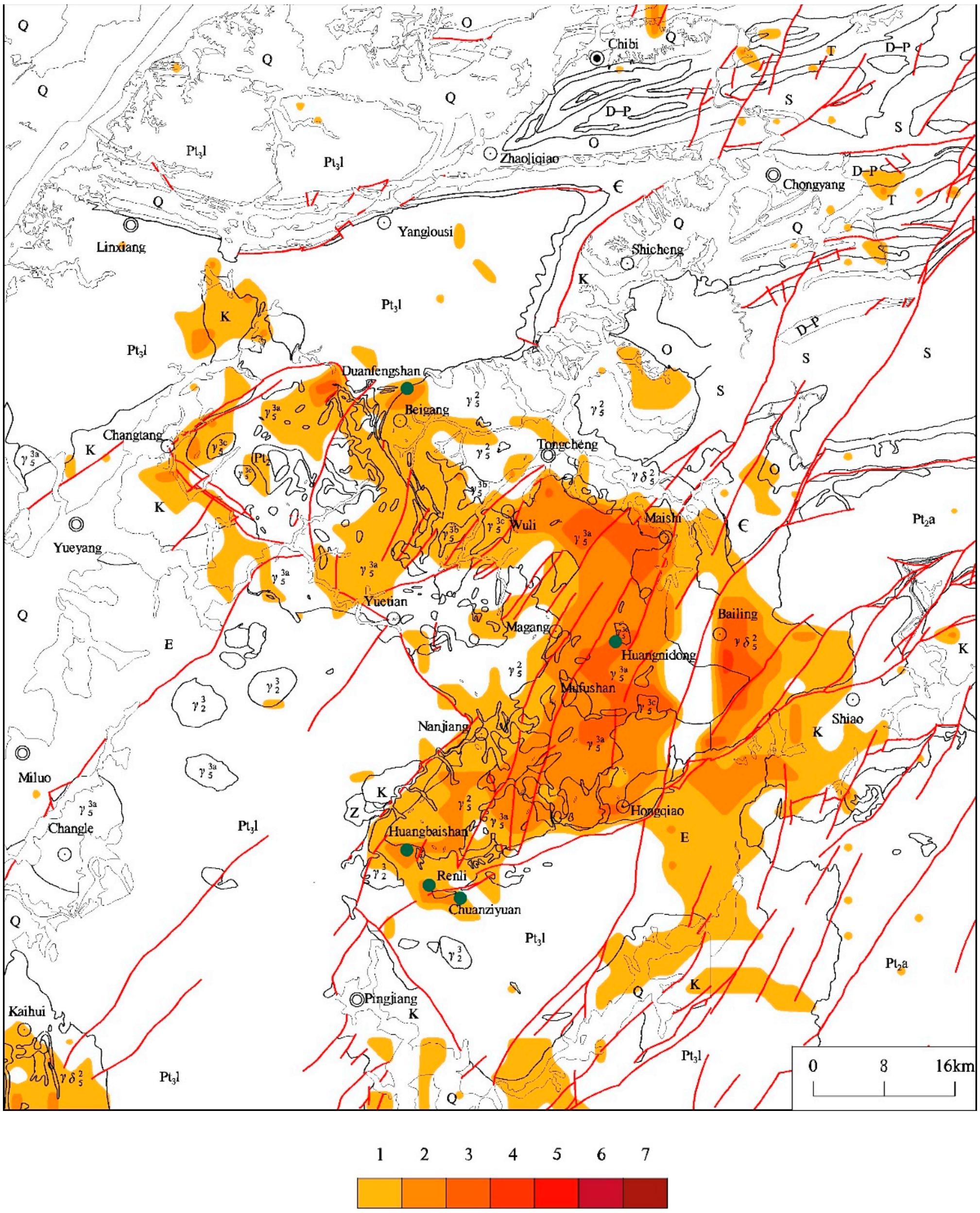

Figure 4. Geochemical anomaly map of Li using the method of seven levels of classification in the Mufushan area.

In Figure 4, the highest anomaly level is only fourth in the method of seven levels of classification. The anomaly areas determined in Figure 4 are mainly relative to the Mufushan granitic complex and the anomaly areas with higher levels are mainly located in the central and eastern areas of the complex. These results indicate that the mineralization of Li in the Mufushan area may have a close relationship with the Mufushan granitic complex genetically.

With respect to the four Li deposits, Huangnidong in the center of the complex is located in the third level area, and the other known Li deposits (Duanfengshan in the northern area, Huangbaishan and Renli–Chuanziyuan in the southwestern area of the complex) are situated in the second level areas. That is to say, all known Li deposits in the study area are located in the anomaly areas of Li, with anomaly levels not less than the second level.

In addition, a fourth anomaly level area is recognized at Bailing in the eastern area of the Mufushan complex. Three other areas with third anomaly level are delineated in the west of Duanfengshan in the north of the complex, Maishi in the eastern area, and Hongqiao in the southern area of the complex. These four anomaly areas are also recognized in the geochemical map of Li with red or grey color tones (Figure 3) and should be surveyed in more detail for resource potential of Li.

4. Conclusions

(1) A fixed-value method is presented to contour the geochemical map of Li with 19 levels and six color tones. This approach is based on lithium concentrations that span from the detection limit to the cut-off grade.

(2) The geochemical map of Li in the Mufushan area is contoured on the new fixed-value method objectively. The results indicate that the majority of the area belongs to the high background area and the known Li deposits are located in the high anomaly areas.

(3) The geochemical anomaly map of Li in the Mufushan area was created using the seven levels of classification method and the results indicate that all known Li deposits fall within the anomaly areas at levels not lower than the second level, and an additional four other areas at levels not lower than the third level are identified as having lithium resource potential.

Author Contributions: P.L. (Peiyu Li): conceptualization, data curation, writing—original draft. S.C., P.L. (Peng Li), J.L., N.L. and X.W. (Xuefeng Wang): data curation, formal analysis. X.W. (Xuan Wu) and X.L.: data curation. Q.G.: conceptualization, methodology, writing—review & editing. All authors have read and agreed to the published version of the manuscript.

Funding: This work was supported by the National Key R&D Program of China (2019YFC0605203), National Natural Science Foundation of China (42330806), and the Geological Survey Project grants from the China Geological Survey (DD20230034).

Institutional Review Board Statement: Not applicable.

Informed Consent Statement: Not applicable.

Data Availability Statement: The raw data supporting the conclusions of this article will be made available by the authors on request.

Acknowledgments: We greatly appreciate the comments from the anonymous reviewers and editors for their valuable suggestions to improve the quality of this manuscript.

Conflicts of Interest: The authors declare no conflicts of interest.

References

1. Dai, H.Z.; Wang, D.H.; Liu, S.B.; Li, X.; Wang, C.H.; Sun, Y. New progress in lithium prospecting abroad (2019~2021) and its significance to China's strategic mining resources exploration. *Acta Geol. Sin.* **2023**, *97*, 583–595.
2. Sovacool, B.K.; Ali, S.H.; Bazilian, M.; Radley, B.; Nemery, B.; Okatz, J.; Mulvaney, D. Sustainable minerals and metals for a low-carbon future. *Science* **2020**, *367*, 6473. [CrossRef] [PubMed]
3. Yu, F.; Wang, D.H.; Yu, Y.; Liu, Z.; Gao, J.Q.; Zhong, J.A.; Qin, Y. The Distribution and Exploration Status of Domestic and Foreign Sedimentary-type Lithium Deposits. *Rock Miner. Anal.* **2019**, *38*, 354–364.
4. Liu, L.J.; Wang, D.H.; Gao, J.Q.; Yu, F.; Wang, W. Breakthroughs of lithium exploration progress (2017~2018) and its significance to China's strategic key mineral exploration. *Acta Geol. Sin.* **2019**, *93*, 1479–1488.
5. Bazamad, M.; Tangsetani, M.H.; Asadi, S.; Staubwasser, M. Investigating the geochemical behavior and exploration potential of lithium in brines; a case study of Bam salt plug, Zagros Zone, southern Iran. *Sci. Rep.* **2023**, *13*, 21567. [CrossRef] [PubMed]
6. Cardoso-Fernandes, J.; Teodoro, A.C.; Lima, A.; Perrotta, M.; Roda-Robles, E. Detecting lithium (Li) mineralizations from space: Current Research and future perspectives. *Appl. Sci.* **2020**, *10*, 1785. [CrossRef]
7. Xu, D.R.; Yu, D.S.; Wang, Z.L.; Li, B.; Chi, G.X.; Zhou, Y.Q.; Zou, S.H.; Deng, T.; Zhang, S.W.; Wang, X.N. Zircon U-Pb and muscovite 40Ar/39Ar dating of Pb-Zn-(Cu) polymetallic deposits in northeastern Hunan Province, Jiangnan Orogen: Evidence for large-scale mineralization in South China at ca. 150–120 Ma. *Ore Geol. Rev.* **2022**, *150*, 105200. [CrossRef]
8. Ye, X.Y.; Li, B.; Chen, X.D.; Lei, J.; Liu, A.H.; Zhao, L.; Li, X.; Tan, D.B.; Xiao, Y.L. Lithium isotopic systematics and numerical simulation for highly-fractionated granite-pegmatite system: Implications for the pegmatite-type rare-metal mineralization. *Ore Geol. Rev.* **2023**, *163*, 105722. [CrossRef]

9. Chen, J.F.; Wen, C.H.; Lv, Z.H.; Huang, J.Z.; Zhang, J.X.; Tang, Y.; Du, Y.; Cao, C.H. Petrogenesis of Mesozoic Li-, Cs-, and Ta-rich (LCT) pegmatites from the Neoproterozoic Jiangnan Orogenic Belt, South China: An alternative origin model for the LCT type pegmatite. *Ore Geol. Rev.* **2023**, *153*, 105276. [CrossRef]
10. Jin, W.; Wan, L.; Tian, Y.; Kusky, T.; Wang, J.; Ke, X.Z.; Yang, J.; Long, W.G. Petrogenesis of early Cretaceous granites in Mufushan complex, northeastern Hunan Province: Insights on middle-late Mesozoic tectonic evolution of eastern South China. *Lithos* **2023**, *456–457*, 107296.
11. Li, P.; Li, J.K.; Chen, Z.Y.; Liu, X.; Huang, Z.B.; Zhou, F.C. Compositional evolution of the muscovite of Renli pegmatite-type rare-metal deposit, northeast Hunan, China: Implications for its petrogenesis and mineralization potential. *Ore Geol. Rev.* **2021**, *138*, 104380. [CrossRef]
12. Xie, X.J.; Cheng, H.X. Sixty years of exploration geochemistry in China. *J. Geochem. Explor.* **2014**, *139*, 4–8. [CrossRef]
13. Xie, X.J.; Mu, X.Z.; Ren, T.X. Geochemical mapping in China. *J. Geochem. Explor.* **1997**, *60*, 99–113.
14. Xiang, Y.C.; Mu, X.Z.; Ren, T.X.; Ma, Z.D.; Liu, R.M.; Gong, Q.J.; Wang, M.Q.; Gong, J.Z.; Yang, W.Z.; Yang, Y.; et al. *Application of Geochemical Survey Data on Potential Evaluation of Mineral Resources in China*; Geological Publishing House: Beijing, China, 2018; pp. 1–445.
15. Li, M.; Xi, X.H.; Xiao, G.Y.; Cheng, H.G.; Yang, Z.F.; Zhou, G.H.; Ye, J.Y.; Li, Z.H. National multi-purpose regional geochemical survey in China. *J. Geochem. Explor.* **2014**, *139*, 21–30. [CrossRef]
16. Xie, X.J. Geochemical Mapping-Evolution of Its Aims, Ideas and Technology. *Acta Geol. Sin.* **2008**, *82*, 927–937.
17. Yousefi, M.; Carranza, E.J.M. Prediction–area (P–A) plot and C–A fractal analysis to classify and evaluate evidential maps for mineral prospectivity modeling. *Comput. Geosci.* **2015**, *79*, 69–81. [CrossRef]
18. Zuo, R.G.; Xiong, Y.H.; Wang, J.; Carranza, E.J. Deep learning and its application in geochemical mapping. *Earth Sci. Rev.* **2019**, *192*, 1–14. [CrossRef]
19. Zuo, R.G.; Carranza, E.J.; Wang, J. Spatial analysis and visualization of exploration geochemical data. *Earth Sci. Rev.* **2016**, *158*, 9–18. [CrossRef]
20. An, Y.L.; Yan, T.T.; Gong, Q.J.; Wang, X.Q.; Huang, Y.; Zhang, B.M.; Yin, Z.Q.; Zhao, X.F.; Liu, N.Q. Chromium (Cr) geochemical mapping based on fixed-values' method: Case studies in China. *Appl. Geochem.* **2022**, *136*, 105168. [CrossRef]
21. Xu, S.C.; Li, J.; Zhang, X.B.; Huang, Z.; Huang, Y.; Long, Y.J.; Xu, Y.Q.; Song, X.F.; Chen, Z.; Li, Y.B.; et al. Tin (Sn) geochemical mapping based on fixed-value method: A case illustration in Gejiu area, Southwest China. *Appl. Sci.* **2024**, *14*, 1765. [CrossRef]
22. Gong, Q.J.; Li, J.Z.; Xiang, Y.C.; Liu, R.M.; Wu, X.; Yan, T.T.; Chen, J.; Li, R.K.; Tong, Y.K. Determination and classification of geochemical anomalies based on backgrounds and cutoff grades of trace elements: A case study in South Nanling Range, China. *J. Geochem. Explor.* **2018**, *194*, 44–51. [CrossRef]
23. Chen, S.Y.; Gong, Q.J.; Li, P.Y.; Xu, S.C.; Liu, N.Q. Describing geochemical backgrounds of lithium in rock-soil-sediment systems. *Appl. Geochem.* **2024**, *162*, 105908. [CrossRef]
24. Gong, Q.J.; Deng, J.; Jia, Y.J.; Tong, Y.K.; Liu, N.Q. Empirical equations to describe trace element behaviors due to rock weathering in China. *J. Geochem. Explor.* **2015**, *152*, 110–117. [CrossRef]
25. Madayipu, N.; Li, H.; Algeo, T.J.; Elatikpo, S.M.; Heritier, R.N.; Zhou, H.X.; Zheng, H.; Wu, Q.H. Long-lived Nb-Ta mineralization in Mufushan, NE Hunan, South China: Geological, geochemical, and geochronological constraints. *Geosci. Front.* **2023**, *14*, 101491. [CrossRef]
26. Wan, L.; Jin, W.; Tian, Y.; Kusky, T.; Ke, X.Z.; Wang, J.; Yang, J.; Long, W.G. Petrogenesis of late Jurassic Mufushan high-Mg diorites and late Mesozoic tectonic evolution of the eastern South China Block. *Gondwana Res.* **2023**, *121*, 118–146. [CrossRef]
27. Wang, L.X.; Ma, C.Q.; Zhang, C.; Zhang, J.Y.; Marks, M. Genesis of leucogranite by prolonged fractional crystallization: A case study of the Mufushan complex, South China. *Lithos* **2014**, *206–207*, 147–163. [CrossRef]
28. Shen, C.B.; Hu, D.; Min, K.; Yang, C.Q.; Zeng, X.W.; Fu, H.Y.; Ge, X. Post-Orogenic Tectonic Evolution of the Jiangnan-Xuefeng Orogenic Belt: Insights from Multiple Geochronometric Dating of the Mufushan Massif, South China. *J. Earth Sci.* **2020**, *31*, 905–918. [CrossRef]
29. Li, Z.H.; Zheng, H.; Li, H.; Zhou, H.X.; Chen, S.F.; Madayipu, N.; Maulana, A.; Wu, Q.H. Polyphase deformation-controlled giant Renli Nb–Ta deposit, South China: Constraints from systematic structural analysis. *Ore Geol. Rev.* **2023**, *153*, 105286. [CrossRef]
30. Hosseini-Dinani, H.; Mokhtari, A.R.; Shahrestani, S.; Vivo, B.D. Sampling Density in Regional Exploration and Environmental Geochemical Studies: A Review. *Nat. Resour. Res.* **2019**, *28*, 967–994. [CrossRef]
31. *DZ/T 0258-2014*; Specifications of Multi-Purpose Regional Geochemical Survey (1:250000). Ministry of Land and Resources of the People's Republic of China: Beijing, China, 2014.
32. Hou, Q.Y.; Yang, Z.F.; Yu, T.; Xia, X.Q.; Cheng, H.X.; Zhou, G.H. *Soil Geochemical Parameters in China*; Geological Publishing House: Beijing, China, 2020; pp. 1–3172.
33. Wen, H.J.; Luo, C.G.; Du, S.J.; Yu, W.X.; Gu, H.N.; Ling, K.Y.; Cui, Y.; Li, Y.; Yang, J.H. Carbonate-hosted clay-type lithium deposit and its prospecting significance. *Chin. Sci. Bull.* **2020**, *65*, 53–59. [CrossRef]
34. *DZ/T 0203-2002*; Specifications for Rare Metal Mineral Exploration. Ministry of Land and Resources of the People's Republic of China: Beijing, China, 2003.

35. Xiong, Y.W.; Qi, H.W.; Hu, R.Z.; Xiao, Y.L.; Wei, L.Y. Lithium isotope behavior under extreme tropical weathering: A case study of basalts from the Hainan Island, South China. *Appl. Geochem.* **2022**, *140*, 105295. [CrossRef]
36. Babechuk, M.G.; Widdowson, M.; Kamber, B.S. Quantifying chemical weathering intensity and trace element release from two contrasting basalt profiles, Deccan Traps, India. *Chem. Geol.* **2014**, *363*, 56–75. [CrossRef]